Microstructure and mechanical properties of selective laser melted Ti-3Al-8V-6Cr-4Zr-4Mo compared to Ti-6Al-4V

C. Madikizela[a,b,*], L.A. Cornish[a], L.H. Chown[a] and H. Möller[c]

[a] School of Chemical and Metallurgical Engineering, and DST-NRF Centre of Excellence in Strong Materials, University of the Witwatersrand, South Africa

[b] National Laser Centre, Council for Scientific and Industrial Research, South Africa

[c] Department of Materials Science and Metallurgical Engineering, University of Pretoria, South Africa

* Corresponding author. Email: Cmadikizela@csir.co.za

Abstract

Beta Ti-alloys are known for their high fracture toughness and ductility, and are used in applications where these properties are needed, such as the aerospace and biomedical industries. The selective laser melting of the alpha + beta Ti-6Al-4V alloy has been extensively studied for applications in the aerospace industry. Although there has been success in building small parts, the acicular α′ microstructure becomes a problem when large parts ($800 \times 400 \times 500\ mm^3$) are built. The acicular α′ microstructure of Ti-6Al-4V causes low fracture toughness and low ductility (<10% elongation), which causes the parts to warp and delaminate from the base plate, even before completion, due to the stress build-up. This work investigated the microstructure and mechanical properties of the beta titanium alloy Ti-38644 and two-phase Ti-6Al-4V in the as-built condition, using scanning electron microscopy with electron backscattered diffraction imaging, optical microscopy, micro-Vickers hardness and tensile tests. Ti-6Al-4V had a fine martensitic α′ structure inside columnar β grains, whereas Ti-38644 had a fully β microstructure, resulting in lower strength. The percentage elongation of Ti-38644 was thrice that of Ti-6Al-4V, showing potential for building large parts.

Keywords: Aerospace; Titanium beta alloys; Selective laser melting; Ductility

1. Introduction

Ti-6Al-4V is a titanium alpha-beta (α + β) alloy currently used in making parts for the aerospace industry [12]. The CSIR-National Laser Centre encountered problems building large Ti-6Al-4V parts ($800 \times 400 \times 500\ mm^3$) by additive manufacturing from powder using the high power, high speed Aeroswift™ selective laser melting (SLM) machine. The higher powers and speeds used by Aeroswift™ tend to induce more residual stresses than the smaller SLM machines. The acicular α′ microstructure of Ti-6Al-4V was reported to cause low fracture toughness and low ductility, < 10% elongation [30], where the part was not able

to withstand the residual stresses, and delamination occurred before completion of the additive manufacturing process. Another problem associated with the α′ martensitic microstructure is its susceptibility to intergranular cracking, resulting in brittle fracture [33]. The acicular α′ microstructure is also strongly textured, giving significant anisotropic behaviour, thus causing a large inconsistency in the mechanical properties under external loading along different sample orientations [33].

The β phase is more ductile than α, thus stabilising β by adding β-stabilisers, such as molybdenum, vanadium, tantalum and niobium, increase ductility [13]. During the past two decades, the aerospace industry has been developing β titanium alloys, due to their attractive properties such as light weight, high fracture toughness, good fatigue resistance, high strength, and good potential of increased hardness without adversely affecting ductility (Weiss et al., [32]; [18]). Another industry with greater interest in Ti-β alloys is the biomedical industry. Zhang et al. [34] selectively laser melted Ti-24Nb-4Zr-8Sn (β alloy) for biomedical applications, and reported tensile strength of 665 MPa and an elongation of 14%. Only β-Ti alloys with biocompatible, non-toxic elements would qualify for these applications. The alloys would also need to have Young's moduli of 10–40 GPa, close to bone [19]. The Young's modulus of Ti-6Al-4V is ~106 GPa, which is too high and would give a mismatch with the surrounding bone, compared to β-Ti alloys that have lower Young's moduli. Despite the numerous advantages of Ti-β alloys, limitations still exist, such as comparatively higher costs, narrower processing windows, intricate processing routes and slightly higher density than α + β alloys [27].

Previously, in situ alloying has been investigated to modify Ti and Ti-6Al-4V by adding β-stabilising elements via the selective laser melting process [14], [15], [31], [6]. All the studies reported undissolved β stabilising elements in the as-built microstructures, which are unlikely to be acceptable in industries with stringent requirements, such as the aerospace industry.

Material development is crucial for the advancement of additive manufacturing technology. To date, investigations have concentrated on manufacturing and testing near-β alloys for the aerospace industry, such as Ti-5Al-5V-5Mo-3Cr (Ti-5553) [26] and Ti-7Mo-3 Nb-3Cr-3Al (Ti-7333) [8] for selective laser melting. The microstructure of Ti-7333 consisted of globular primary alpha α_p and fine lenticular secondary alpha α_s distributed in a β matrix [8], while the Ti-5553 alloy consisted of β grains growing parallel to the build direction [26]. The Ti-7333 alloy [8] had a more desirable combination of tensile strength (1427 MPa) and ductility (14%) than Ti-5553 [26], which had the same elongation but a lower tensile strength of 800 MPa.

The selective laser melting of commercial β alloys has not been extensively studied, mainly due to the lack of availability of these alloys as powders [9]. Beta-Ti alloys are more readily heat treatable to increase the hardness than α and α + β alloys [17].

Beta-Ti alloys have been identified as the best candidates for producing landing gear beams for the aerospace industry [2], [5]. They give the best trade-off between the two most important considerations in landing gear beams: maximising specific strength and fatigue strength [2]. The Ti-3Al-8V-6Cr-4Zr-4V β alloy has a good combination of strength and ductility which is suitable for use in aircraft manufacture. Properties such as high cycle fatigue and fracture toughness can be customised by performing cold work, followed by solution annealing and aging to precipitate α and form a microstructural gradient, where the hardness near the surface is high, without modifying the hardness of the bulk material [2].

Producing this alloy via SLM with better mechanical properties than either forged or additively manufactured Ti-6Al-4V could make it suitable for aerospace applications. In this work, the microstructure and mechanical properties of the more ductile Ti-3Al-8V-6Cr-4Zr-4Mo (Ti-38644) were compared to Ti-6Al-4V.

2. Materials and methods

Ti-38644, with composition 74% Ti, 5% Al, 8% V, 6% Cr, 4% Zr and 4% Mo (mass %), was procured in rod form from Titanium A to Z (United States) and then spherically gas atomised by TLS Technik, Germany. Ti-6Al-4V, with composition 90% Ti, 6% Al and 4% V (mass %), was readily available as spherical powder from TLS Technik, Germany. The particle size of the Ti-38644 β-Ti alloy was 20–80 μm with a d_{50} of 70 μm, while Ti-6Al-4V had a particle size of 50–100 μm with a d_{50} of 76 μm. Secondary electron imaging (SEI) SEM images of the powders are shown in Fig. 1.

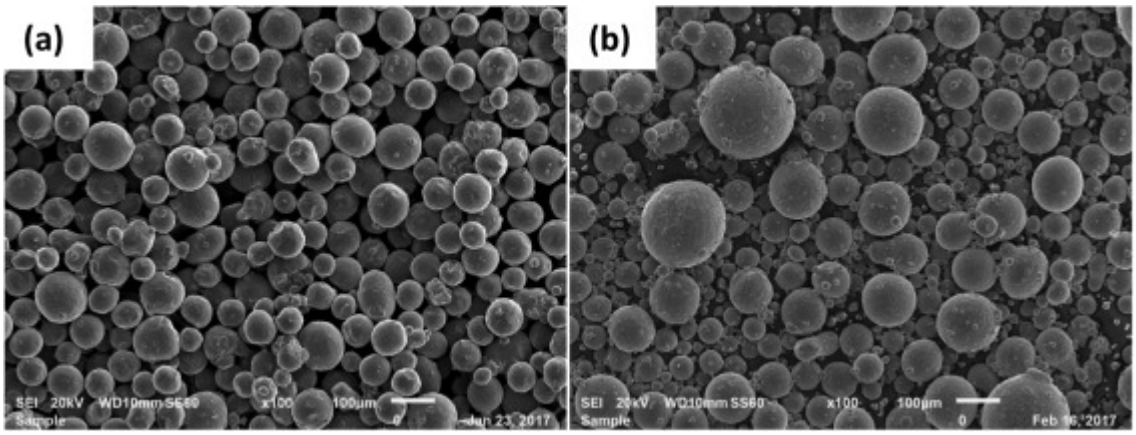

Fig. 1. SEM-SEI images of the powders: (a) Ti-6Al-4V powder, and (b) Ti-36844 powder.

Samples were processed with a Nd:Yag laser at 1.3 kW power and at a speed of 4 m/s with a hatch overlap of 65%, allowing the manufacture of samples with densities > 98% (evaluated by image analysis). The dimensions of cubic samples for microstructural analysis were $10 \times 10 \times 10$ mm^3 (Fig. 2a), and the dimensions of the blocks prior to machining the tensile samples were $12 \times 56 \times 3$ mm^3 (Fig. 2b). The samples were prepared metallographically and etched with Kroll's reagent for optical microscopy, then studied using scanning electron microscopy (SEM) with energy dispersive X-ray spectroscopy (EDX), and electron backscatter diffraction (EBSD). Micro-Vickers hardness tests were done using a 300 g load and a dwell time of 10 s, and the average of 20 results was obtained. Tensile samples of Ti-6Al-4V and Ti-38644 were machined into 'dog bone' specimens and the tensile tests were performed according to the ASTM E8 M standard [3]. Average results were obtained from four tensile tests for each alloy.

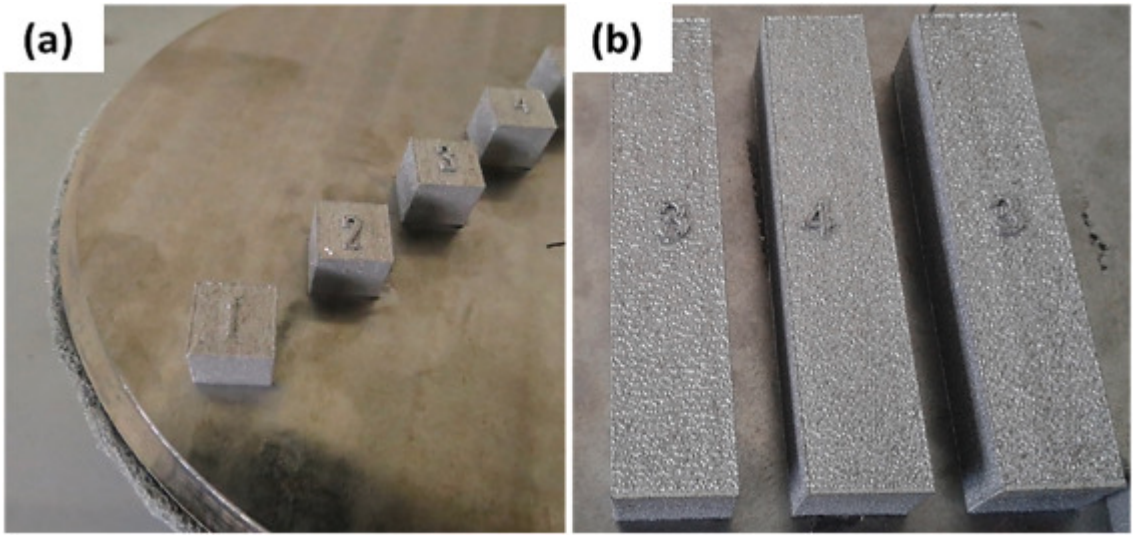

Fig. 2. Photographs of samples built on a SLM platform: (a): 10 × 10 × 10 mm^3 cubes for microstructural analysis, (b) 56 × 12 × 6 mm^3 rectangular samples for machining tensile test samples.

3. Results and discussion

3.1. Microstructure

Fig. 3a shows a cross-section of the microstructure of Ti-6Al-4V produced via SLM. There were columnar grains in the build direction through multiple layers. These grains were due to the partial re-melting of the previously fused layers, which led to epitaxial growth [30], [31], [33]. There was also a needle-like structure within the columnar grains (Fig. 3a). The microstructure of Ti-6Al-4V was martensitic, mostly due to the high temperature gradients used during SLM, as found by Murr et al. [20] and Thijs et al. [30]. Conversely, Fig. 3b and 5 show that the microstructure of the Ti-38644 alloy consisted of shorter columnar β grains running parallel to the build direction. According to Thijs et al. [30], Vrancken et al. [31] and Schwab et al. [26], these elongated grains also grew by epitaxial growth, where the previously solidified layer acted as nucleation sites. This behaviour was typical of samples manufactured by the SLM process.

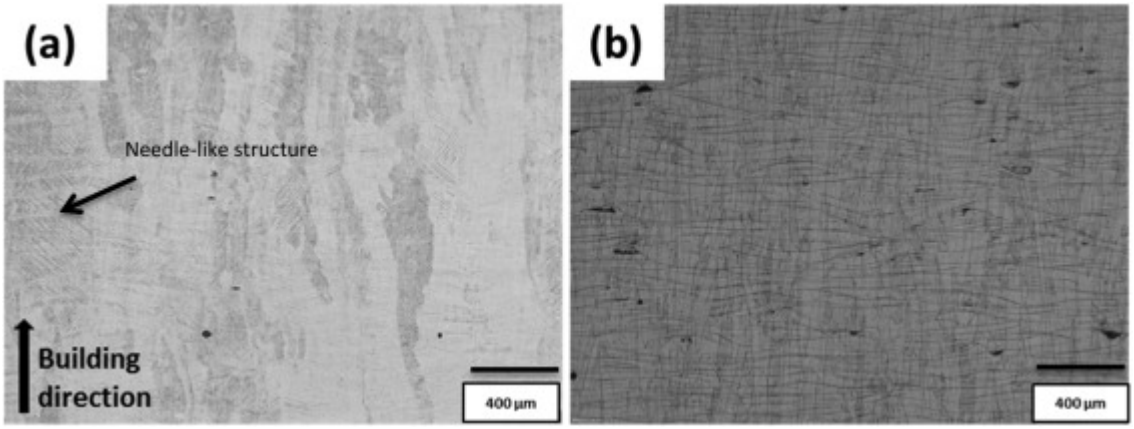

Fig. 3. Optical micrographs showing the microstructures of samples built via SLM: (a) Ti-6Al-4V, and (b) Ti-38644.

Wave-like structures were also present in the β-Ti microstructure. Vrancken et al. [31] interpreted this structure as the melt pool boundaries. This has been shown to be characteristic of more ductile material than Ti-6Al-4V, which does not exhibit this phenomenon [14], [25], [31], [6]. Alloys with higher ductility are more viscous, creating a more volatile melt pool, and the high cooling rates also favour the creation of these boundaries [14], [15], [31], [9].

Ti-6Al-4V only has vanadium as a β-stabilizing element, whereas Ti-38644 also has molybdenum and chromium as β-stabilisers, together with vanadium. Aluminium was the only α-stabilising element in the Ti-38644 alloy. Vrancken et al. [31] reported that Zr destabilised the planar solidification front, without affecting the α and β phases, which likely explains its role in Ti-38644. The higher proportion of β-stabilisers than α-stabilisers in Ti-38644 allowed for more of the β phase to be stabilized than in Ti-6Al-4V.

Phase analysis by EBSD (Fig. 4) identified α-Ti as the major phase in Ti-6Al-4V. Due to the hexagonal α-Ti in the microstructure, the type of α-Ti present was deduced to be α′.

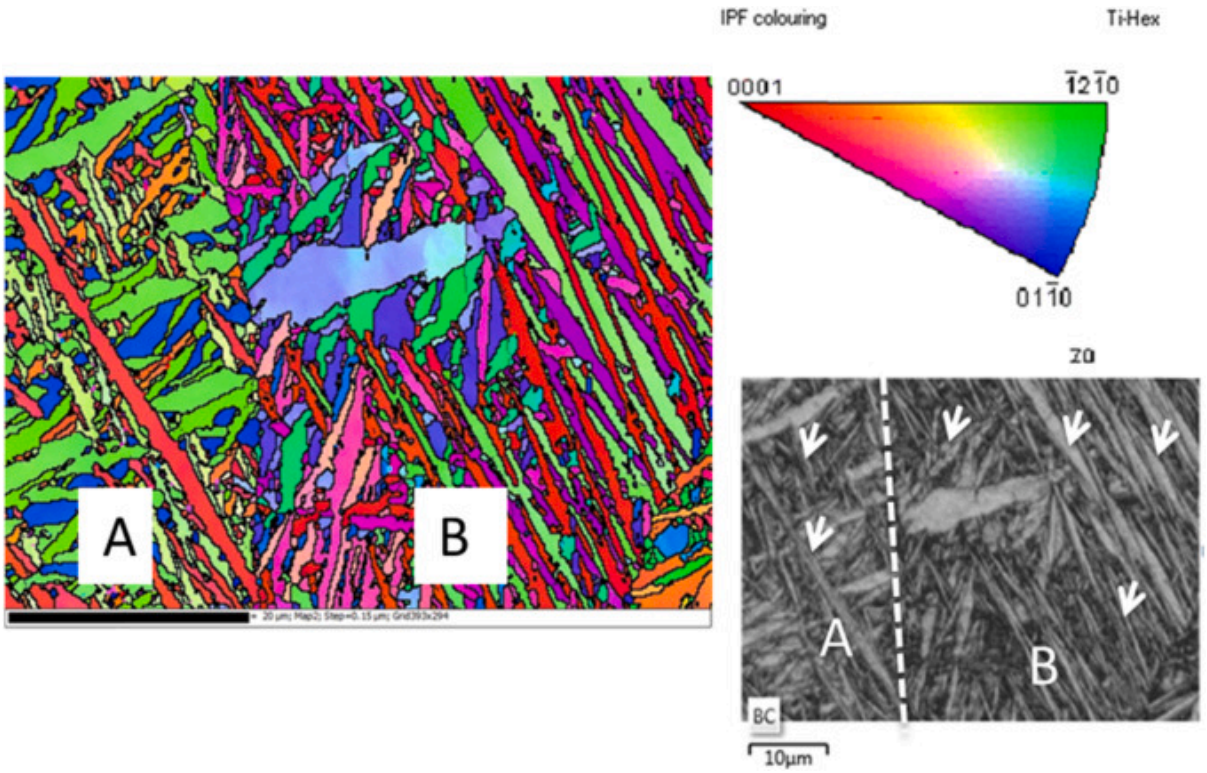

Fig. 4. EBSD IPF orientation map and band contrast image taken in the z direction of the Ti-6Al-4V sample.

From the inverse pole figure (IPF) (Fig. 4), α grains appeared to have precipitated randomly within the β grain boundaries as indicated by the white arrows. This was identified as typical of the martensitic transformation, as the α′ grains formed simultaneously at different locations inside the β grains [29]. From the grain orientation map (Fig. 4), there were regions where α′ needles were aligned in the same direction, and also regions where the needles grew at angles between ~60° and 90° to the other set, forming a “basket-weave” microstructure. This growth form was due to the competitive growth of α′ needles [28]. The α′ needles differed in width, and some also appeared longer, limited by the grain size and the space available for growth. In addition, the α′ needle size differences have been attributed to the build platform acting as

a heat sink, therefore promoting variations in the grain growth of these α′ needles [29]. This result is consistent with other work involving the SLM of Ti-6Al-4V ([31], [29]). No explanation has yet been given for the preferred arrangement of α′ martensitic laths [4,29]), but it is likely to reduce the energy. However, from the inverse pole figure (Fig. 4), the direction in which the α′ grains grew depended on the β grain shapes. Most of the α′ grains in β grain A were depicted as green, indicating a strong 1210 orientation. The other dominant colours were blue and orange, indicating a strong 0110 and ~0001 orientation respectively. Conversely, β grain B had grains with colours ranging from red to blue, indicating that the crystal direction parallel to the z direction of the sample was between the 0001 and 0110 directions. From the phase analysis, α′ was identified as the major phase.

The phase analysis by EBSD of Ti-38644 (Fig. 5) identified β-Ti as the only phase. Fig. 5 shows there were regions in the microstructure which had rounded grains clustered together, i.e. the grains were globular and equiaxed. Schwab et al. [26] deduced that the change in solidification morphology from planar to cellular and cellular-dendritic structures was due to the destabilization of the planar solidification, due to the changing ratio of the thermal gradient and solidification rate. The IPF (Fig. 5) shows that most of the grains were depicted as red to pink, indicating a strong orientation between the 001 and 111 directions. For undercooled melts, crystallization occurs in the “easy growth” directions and for bcc cubic crystal structures this is the

direction [25]. This growth direction corresponds to the direction of the maximum temperature gradient, which is generally in the build direction in laser additive manufactured material [9]. Green was the other dominant colour depicted for the β grains, indicating a strong 101 orientation.

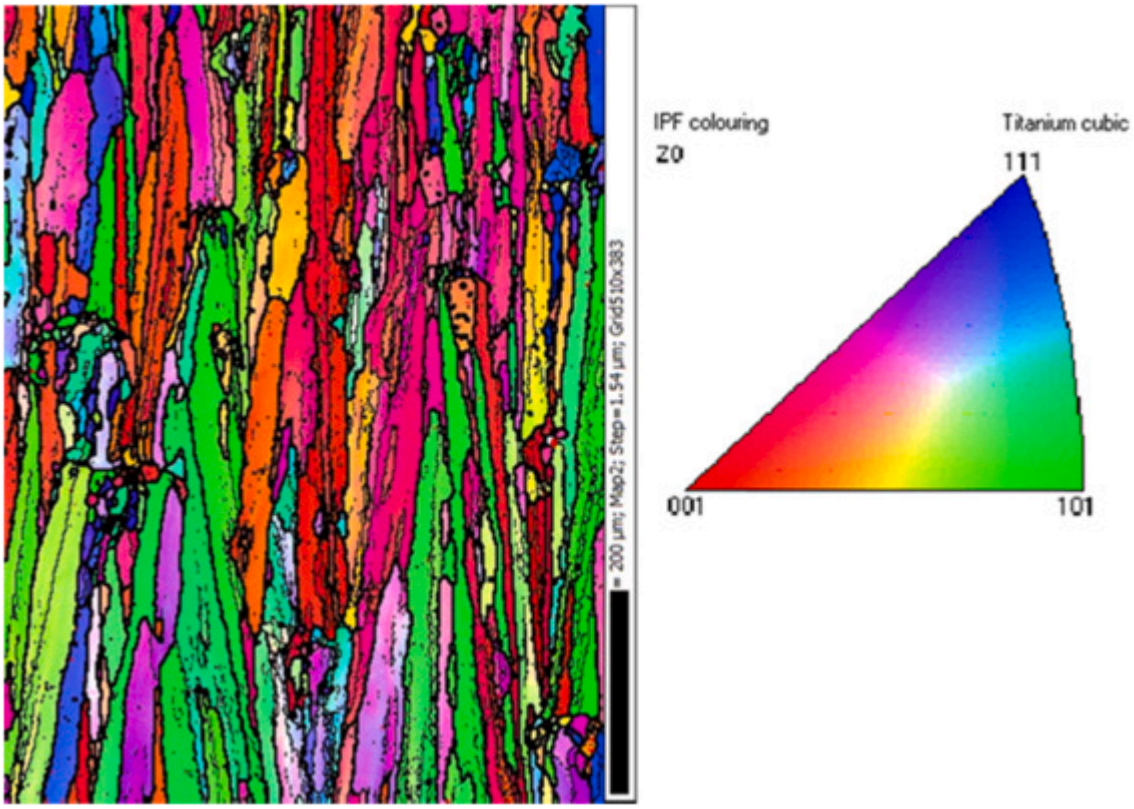

Fig. 5. EBSD IPF orientation map taken in the z direction of the Ti-38644 sample. (For interpretation of the references to color in this figure, the reader is referred to the web version of this article).

Fig. 6 shows the grain size analysis done on Ti-6Al-4V and Ti-38644 expressed in length (Figs. 6a and c) and width (Figs. 6b and d) of the grains. Figs. 6a and b show that most of the Ti-6Al-4V grains were below 3 µm long, with a width below 1 µm. Agius et al. [1] reported α′ grains with widths of 1–3 µm for as-built Ti-6Al-4V produced by SLM, and Thijs et al. [30] reported columnar β grains ~100 µm long, for as-built SLM produced Ti-6Al-4V.

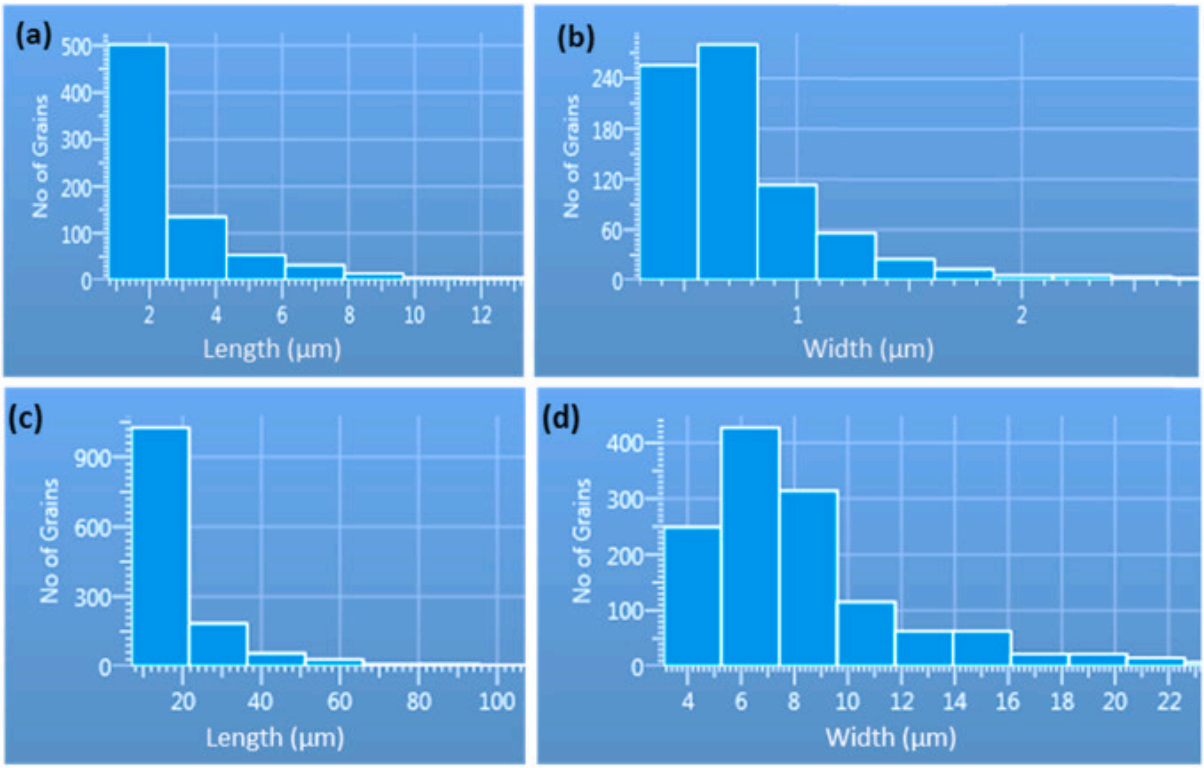

Fig. 6. EBSD grain size histograms: (a) length (µm) for Ti-6Al-4V α grains, and (b) width (µm) for Ti-6Al-4V α grains (c) length (µm) for Ti-38644 β grains, (d) width (µm) for Ti-38644 β grains.

Fig. 6c shows that most of the Ti-38644 grains were shorter than 20 µm. The layer thickness was kept at 50 µm, so most of the grains were smaller than the layer thickness. Fig. 6d shows that most of the Ti-38644 grains had widths of 4–10 µm. Schwab et al. [26] reported elongated grains up to 100 µm growing across the melting border for the as-built SLM Ti-5553. The grains for Ti-38644 were smaller than this, due to the difference in material and manufacturing speed. Schwab et al. [26] used slow speeds, ranging from 100 to 180 mm/s, while the speed used in this work was 4000 mm/s. The higher speeds promoted faster cooling, and therefore a more refined microstructure.

3.2. Mechanical properties

Fig. 7 shows the stress-strain curves for Ti-6Al-4V and Ti-38644. The area under a stress-strain curve gives an indication of a material's fracture toughness [23], and were calculated using the trapezium rule in Eq. (1) [21]:(1)

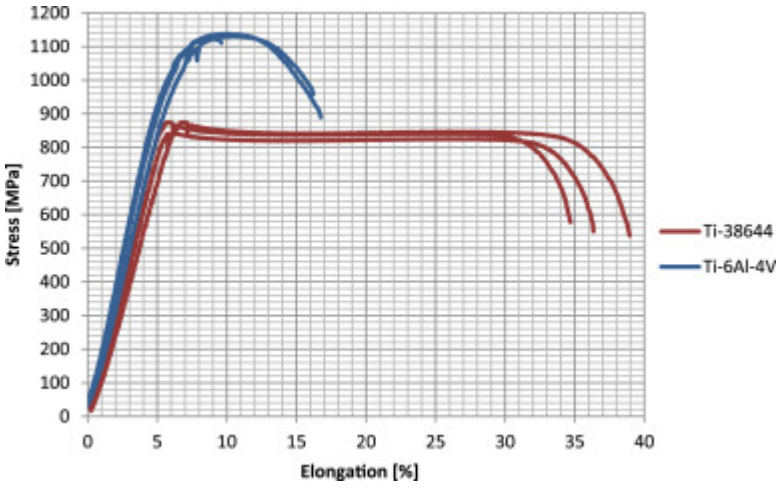

Fig. 7. Stress-strain curves for Ti-6Al-4V (blue) and Ti-38644 (red).

For Ti-6Al-4V, this area was calculated to be 2803.3 mm^2, whereas for the β-Ti alloy, the area was 5454.3 mm^2. Thus, Ti-38644 had a larger area under the curve than Ti-6Al-4V and thus a higher fracture toughness than Ti-6Al-4V. The fracture toughness and strength are usually inversely proportional [7], so high fracture toughness would be associated with a decrease in strength. The best microstructure for a good balance of strength and toughness is one strengthened with fine particles spaced sufficiently widely, so that the strain fields do not overlap [7]. These particles must be small and well bonded to the matrix [7]. Although Ti-38644 does not have the ideal microstructure for high fracture toughness, the presence of the β phase and the elongated grains gave a high fracture toughness that would allow the material to withstand stresses better than Ti-6Al-4V during manufacturing.

Table 1 shows measured selected mechanical properties of Ti-6Al-4V and Ti-38644. The hardness of Ti-38644 (309 ± 9 $HV_{0.3}$) was lower than Ti-6Al-4V (360 ± 9 $HV_{0.3}$). This was expected, since Ti-6Al-4V had a fine martensitic structure and Ti-38644 was single phase β. The fine structure of Ti-6Al-4V led to higher strength, due to more grain boundary strengthening (because there were more grain boundaries from the finer grains) according to the Hall-Petch relationship [10], [11]. As noted earlier, the β-grain size of the Ti-38644 alloy (~20 μm) was lower than the typical β-grain size of Ti-6Al-4V (~100 μm). This should have increased the strength, since smaller grains usually have higher dislocation densities [24]. However, due to the presence of the fine ά in Ti-6Al-4V, its strength was much higher than Ti-38644, which only had β grains. Additionally, the crystal structure of bcc β is softer than hcp α, having more slip planes at different orientations [7]. The 0.2% proof stress and ultimate tensile strength (UTS) of Ti-6Al-4V were higher than for Ti-38644, and the elongation of Ti-38644 was higher than for Ti-6Al-4V.

Table 1. Selected mechanical tests results, compared with other alloys.

	Vickers Hardness	**E (GPa)**	**0.2% Proof stress (MPa)**	**UTS (MPa)**	**Elongation (%)**
Ti-6Al-4V	360 ± 9	106.9 ± 2.9	962.6 ± 2.0	1130.5 ± 7.0	9.0 ± 3.0
Ti-38644	309 ± 10	68.3 ± 5.0	845.1 ± 1.0	863.4 ± 2.0	30.5 ± 3.0
Ti-24 Nb− 4Zr-8Sn [34]	240 ± 1	53 ± 1	563 ± 38	665 ± 18	13.8 ± 4.1
Ti− 6Al-4V+10Mo [31]	338 ± 5	73 ± 1	858 ± 16	919 ± 10	20.1 ± 2.0

Comparing Ti-38644 with another SLM processed β alloy, Ti-24 Nb-4Zr-8Sn [34], Ti-38644 had superior mechanical properties with a good combination of strength and ductility. The β alloy made by in situ alloying of Ti-6Al-4V with 10 wt% Mo [31] had a slightly higher strength (919 ± 10 MPa) than Ti-38644 (863.4 ± 2.0 MPa), and lower ductility (20.1 ± 2.0% compared to 30.5 ± 3.0%). Even though the in situ alloyed material had higher fracture toughness and ductility, for high power, high speed processing, inhomogeneities resulting from unmelted and partially melted Mo powder in the Ti-6Al-4V matrix gave micro-galvanic corrosion effects, as recognized by Madikizela et al. [16]. Therefore, using a pre-alloyed material eliminates these issues, making it a better option than in situ alloying, especially for industries with stringent requirements such as the aerospace industry.

In SLM processing, it is common to have different tensile properties in different directions, i.e. anisotropy [7]. The properties most affected by a change in orientation are the yield strength, and to some extent, the tensile strength [7]. The tensile samples in the current work were built in the XY direction (longitudinal direction). Horizontally built (XY) samples exhibit higher strengths and lower ductility than vertically built (XZ) samples in tensile testing [22], [29]. Therefore, the elongation could have been higher than 30% if the samples had been built in the XZ and ZX directions, and the strength could have been lower. Simonelli et al. [29] deduced that the lower elongations in the XY direction than for the XZ and ZX directions could have been due to the samples having more defects (voids). Curling of SLM parts is caused by thermal stresses, which are higher in samples built in the XY direction, and curling leads to uneven powder deposition, which causes pores [29]. Therefore, samples also need to be built in the ZX and XZ directions to compare the tensile properties with samples built in the XY direction.

Fig. 8 shows the fracture surfaces of the alloys. Fig. 8a shows that Ti-6Al-4V had a mixture of different sized dimples, indicating ductile fracture, and smooth areas indicating regions of brittle fracture. Fig. 8b shows that Ti-38644 had deeper dimples which covered the whole fracture surface, indicating ductile fracture. However, ductile fracture was the major fracture mode seen on the fracture surfaces for both alloys. Xu et al. [33] associated elongated prior β grains and the acicular α′ martensite of Ti-6Al-4V with intergranular failure. The elongation of Ti-6Al-4V was below 10%, and therefore as-built SLM-produced Ti-6Al-4V would not qualify for use in critical structural applications [33].

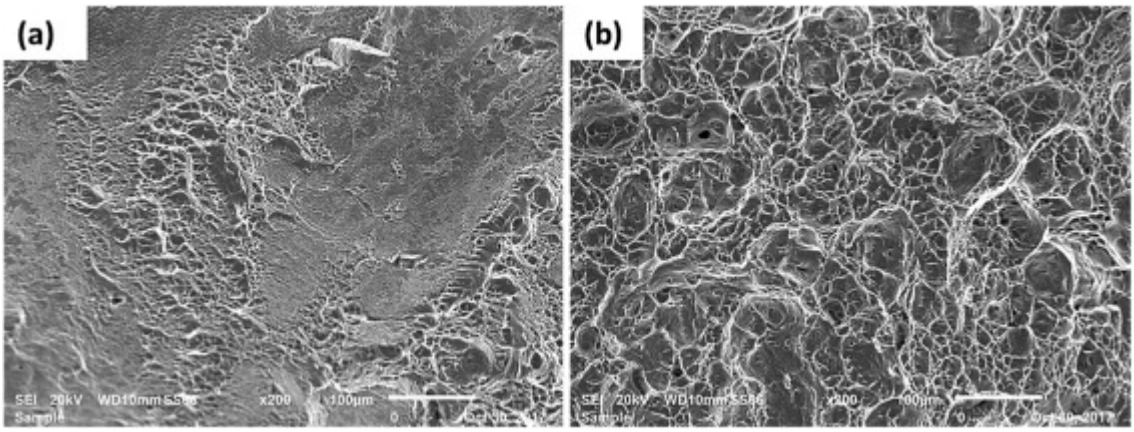

Fig. 8. SEM-SE images of the fracture surfaces of: (a) Ti-6Al-4V and (b) Ti-38644.

4. Conclusions

The microstructure of Ti-38644 was fully β, and the grains were elongated in the building direction. The strength of Ti-6Al-4V was attributed to the fine α′ microstructure, while the thicker but shorter β grains in Ti-38644 promoted higher ductility and fracture toughness. This indicates that Ti-38644 would be better suited for making larger parts in high power, high speed processing, as it should be able to withstand the residual stresses which caused the Ti-6Al-4V parts to delaminate. This work contributed to the available knowledge, showing that Ti-38644 could be used for additive manufacturing. Its microstructure and mechanical properties gave promising results, not only for high power, high speed processing, but for additive manufacturing in general. The use of pre-alloyed powder was demonstrated to be better suited than in situ alloying as it produced a homogeneous microstructure for SLM.

Data availability

The raw/processed data required to reproduce these findings cannot be shared at this time as the data also forms part of an ongoing study.

Acknowledgements

The authors thank the CSIR (Council for Scientific and Industrial Research, South Africa) and the Department of Science and Technology, South Africa for funding this project.

References

[1] D. Agius, K.I. Kourousis, C. Wallbrink, A review of the as-built SLM Ti-6Al-4V mechanical properties towards achieving fatigue resistant designs, Metals 8 (75) (2018), https://doi.org/10.3390/met8010075.
[2] R.A. Antunes, C.A.F. Salvador, M.C.L. DE Oliveira, Materials selection of optimized titanium alloys for aircraft applications, Mater. Res. 2 (21) (2018) e20170979.
[3] ASTM INTERNATIONAL, 2009. Standard Test Methods for Tension Testing of Metallic Materials. American Association State Highway and Transportation Officials Standard AASHTO No T68, USA.
[4] D. Banerjee, J.C Williams, Perspectives on Titanium Science and Technology, Acta Mater. 61 (3) (2013) 844–879.
[5] R.R. Boyer, Titanium for aerospace: rationale and applications, Adv. Perform. Mater. 2 (1995) 349–368.
[6] E. Chlebus, B. Kuznicka, R. Dziedzic, T. Kurzynowski, Titanium alloyed with rhenium by selective laser melting, Mater. Sci. Eng. A 620 (2015) 155–163.
[7] G.E. Dieter, Mechanical Metallurgy, McGraw-Hill Book Co., Singapore, 1988, pp. 322–323.
[8] J. Fan, J. Li, H. Kou, K. Hua, B. Tang, Y. Zhang, Microstructure and mechanical property correlation and property optimization of near β titanium alloy Ti-7333, J. Alloy. Compd. 682 (2016) 517–524.
[9] M. Fischer, D. Joguet, G. Robin, L. Peltier, P. Laheurte, In situ elaboration of a binary Ti–26Nb alloy by selective laser melting of elemental titanium and niobium mixed powders, Mater. Sci. Eng. C 62 (2016) 852–859.
[10] E.O. Hall, The deformation and ageing of mild steel: III, Proc. Phys. Soc. B 64 (1951) 747.

[11] N. Hansen, Hall-Petch relation and boundary strengthening, Scr. Mater. 51 (8) (2004) 801–806.
[12] B. He, W. Wu, L. Zhang, L. Lu, Q. Yang, Q. Long, K. Chang, Microstructure characteristic and mechanical property of Ti6Al4V alloy fabricated by selective laser melting, Vacuum 150 (2018) 79–83.
[13] C. Leyens, M. Peters, Titanium and Titanium Alloys, Wiley Online Library, Germany, 2003.
[14] C. Madikizela, L.A. Cornish, L.H. Chown, H. Moller, D. Louw, Microstructure of in situ alloyed Ti-6Al-4V and 10Mo as a function of process parameters, in: Proceedings of the Frontiers in Optics 2016 Conference, OSA Technical Digest (online), Optical Society of America, Rochester, New York, USA, 17–21 October 2016, Paper FF2C.6, 2016.
[15] C. Madikizela, L.A. Cornish, L.H. Chown, N. Arthur, H. Moller, Comparison of in situ alloyed Ti-6Al-4V+10Mo via selective laser melting and laser metal deposition, in: Proceedings of the 18th Annual International RAPDASA Conference, Durban, South Africa, 8–10 November 2017.
[16] C. Madikizela, L.A. Cornish, L.H. Chown, H. Moller, Micro-galvanic corrosion of Ti-6Al-4V in situ alloyed with molybdenum via selective laser melting, Afr. Corros. J. 4 (1) (2018) 3–7.
[17] J.D. Majumdar, I. Manna, Laser surface engineering of titanium and its alloys for improved wear, corrosion and high-temperature oxidation resistance, Laser Surf. Eng. (2015) 483–521.
[18] P. Manda, A. Pathak, A. Mukhopadhyay, U. Chakkingal, A.K. Singh, Ti-5Al-5Mo-5V-3Cr and similar Mo equivalent alloys: first principles calculations and experimental investigations, J. Appl. Res. Technol. 15 (2017) 21–26.
[19] M.T. Mohammed, Z.A. Khan, A.N. Siddiquee, Beta titanium alloys: the lowest elastic modulus for biomedical applications: a review, Int. J. Mater. Metall. Eng. 8 (8) (2014) (scholar.waset.org/1307-6892/9999146).
[20] L.E. Murr, S.A. Quinones, S.M. Gaytan, M.I. Lopez, A. Rodela, E. Martinez, E.Y. Martinez, D.H. Hernandez, F. Medina, R.B. Wicker, Microstructure and mechanical behavior of Ti–6Al–4V produced by rapid-layer manufacturing, for biomedical applications, J. Mech. Behav. Biomed. Mater. 2 (1) (2009) 20–32.
[21] H. Neill, D. Quadling, J. Gilbey, Cambridge international AS and A Level Mathematics: Pure Mathematics 2 and 3 2 Cambridge University Press, USA, 2016, p. 131.
[22] A.A. Popovich, V. Sufiiarov, Sh, E.V. Borisov, I.A. Polozov, D.V. Masaylo, A.V. Grigoriev, Anisotropy of mechanical properties of products manufactured using selective laser melting of powdered materials, Russ. J. Non-Ferr. Met. 58 (4) (2017) 389–395.
[23] D. Roylance, Stress-Strain Curves, Department of Materials Science and Engineering, Massachusetts Institute of Technology, Cambridge, 2001 (23 August 2001).
[24] G.A. Salishchev, S. Yu Mironov, Effect of grain size on mechanical properties of commercially pure titanium, Russ. Phys. J. 44 (6) (2001) 596–601.
[25] H. Schwab, G.K. Prashanth, L. Löber, U. Kühn, E. Jürgen, Selective laser melting of Ti-45Nb alloy, Metals 5 (2015) 686–694.
[26] H. Schwab, F. Palm, U. Kühn, J. Eckert, Microstructure and mechanical properties of the near-beta titanium alloy Ti-5553 processed by selective laser melting, Mater. Des. 105 (2016) 75–80.
[27] S. Shekhar, R. Sarkar, K.S. Kar, A. Bhattacharjee, Effect of solution treatment and aging on microstructure and tensile properties of high strength β titanium alloy, Ti-5Al-5V-5Mo-3Cr, Mater. Des. 66 (2015) 596–610.
[28] Simonelli, M., Tse, Y. and Tuck, C., 2012. Microstructure of Ti-6Al-4V produced by

selective laser melting, Journal of Physics: Conference Series, 371, Conference no. 1, paper no. 012084.
[29] M. Simonelli, Y. Tse, C. Tuck, Effect of the build orientation on the mechanical properties and fracture modes of SLM Ti-6Al-4V, Mater. Sci. Eng. A, Struct. Mater. Prop. Microstruct. Process. 616 (2014) 1–11.
[30] L. Thijs, F. Verhaeghe, T. Craeghs, J. Van Humbeeck, J. Kruth, A study of the micro-structural evolution during selective laser melting of Ti–6Al–4V, Acta Mater. 58 (9) (2010) 3303–3312.
[31] B. Vrancken, L. Thijs, J. Kruth, J. VAN Humbeeck, Microstructure and mechanical properties of a novel β titanium metallic composite by selective laser melting, Acta Mater. 68 (2014) 150–158.
[32] I. Weiss, S.L. Semiatin, Thermomechanical processing of beta titanium alloys-an overview, Mater. Sci. Eng. A243 (1998) 46–65.
[33] W. Xu, M. Brandt, S. Sun, J. Elambasseril, Q. Liu, K. Latham, K. Xia, M. Qian, Additive manufacturing of strong and ductile Ti–6Al–4V by selective laser melting via in situ martensite decomposition, Acta Mater. 85 (2015) 74–84.
[34] L.C. Zhang, D. Klemm, J. Eckert, Y.L. Hao, T.B. Sercombe, Manufacture by selective laser melting and mechanical behaviour of a biomedical Ti-24Nb-8Sn alloy, Scr. Mater. 65 (2011) 21–24.